

FIG. 1. The effect of cyclohexane level on filament resistance and life.

since TiC is reported to have slightly greater oxidation resistance than Ti.³ Also, as carburization takes place, the change in emittance of the filament surface may be a contributing factor. Although it is well known that carbide formation can occur under these conditions, it may not be obvious to users of glovebox equipment. Based upon these results, it is apparent that the presence of carburizing vapors will seriously affect the accuracy of testers using hot filaments of carbide forming metals.

¹ J. McKee, "An Inert Gas Purity Tester," UNC-SPLM-63 (1965).

² J. McKee in *Proceedings of the Conference on Application of High Temperature Instrumentation to Liquid-Metal Experiments*, ANL-7100, (1965), p. 443.

³ W. W. Webb, John T. Norton, and Carl Wagner, *J. Electrochem. Soc.* **103**, 112 (1956).

Single Mode Output with the Spectra-Physics Model 125 He-Ne Laser*

G. D. CURRIE

*Radar and Optics Laboratory, Willow Run Laboratories,
Institute of Science and Technology, The University of Michigan,
Ann Arbor, Michigan 48107*

(Received 26 May 1969)

THE importance of single mode laser output is well known. It is easy to restrict the He-Ne laser to single transverse mode operation by using an in-cavity aperture. However, when high power operation is desired in long lasers, oscillation occurs in a number of axial modes. This can severely restrict the depth of field available for conventional holography and it limits the distortion-free bandwidth for modulation to a frequency range between 100 kHz and 100 MHz.

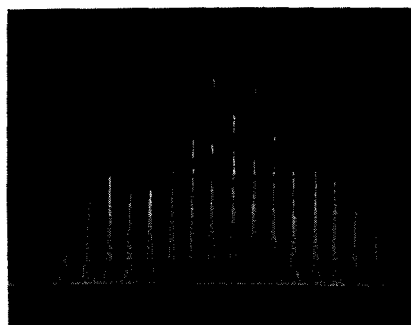


FIG. 1. Multimode laser spectrum. Vertical scale represents intensity in arbitrary units, horizontal scale in units of 150 MHz/div.

Many schemes have been devised to attain single mode oscillation or to reduce the number of axial modes.¹⁻³ One of these is to insert an extra reflector in the cavity. The reflecting element can be an uncoated 15 mm diam flat mirror blank. There is an optimum reflector position which will give single mode output with high efficiency³ (about 94%). However, single mode oscillation at lower output can be attained with the extra mirror at a non-optimum position. We would like to point out that such a position is readily available in the Spectra-Physics model 125 lasers having the model 325 cavity extender. The mirror is inserted in the "inner reflector mount," supplied with the laser. Thus, the extra cost for single mode operation is only that of the mirror blank (about \$35).

A scanning interferometer was used to monitor the optical spectrum of a laser modified in this manner. Figure 1 shows normal multimode operation with 90 mW output power. Figure 2 shows a storage oscilloscope record of the mode history during the first hour after the mode selection mirror was inserted into the cavity (the laser had been running for several hours). In this case the output power was only 16 mW, due to misalignment of the prism mirror. During the first 22½ min the mode drifted by 180 MHz (to the left in the photograph). At the end of this period the mode jumped to a new position. It drifted (still further to the left) by about 100 MHz and then reversed direction. For 37½ min it wandered around in this 100 MHz band. Thus the laser radiation

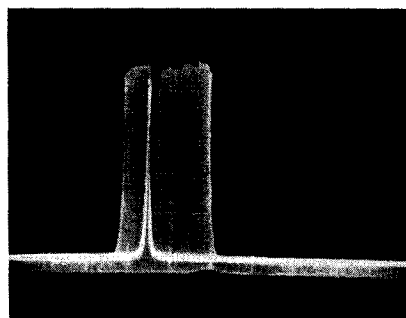


FIG. 2. Storage oscilloscope record of single mode laser output during 1 h period.

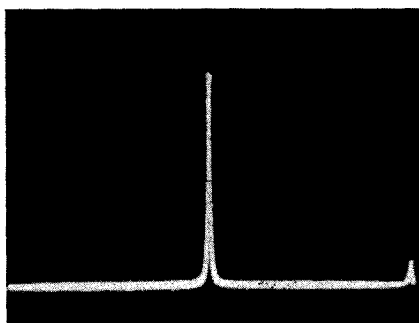


FIG. 3. One minute storage oscilloscope record of single mode laser spectrum.

had an effective holographic coherence length of 3 m for the entire period. Figure 3 was made about $\frac{1}{2}$ h after Fig. 2 and after the output power had been maximized, at 36 mW, by adjustment of the prism. This figure shows a storage oscilloscope display of the behavior of the spectrum over a period of 1 min. It is apparent that the frequency deviation was within the instrumental bandwidth (10 MHz) of the optical spectrum analyzer. The corresponding coherence depth was 30 m.

* This work was sponsored by the USAF Avionics Laboratory, Wright-Patterson Air Force Base, Ohio, under Contract No. F 33-615-67C-1814.

¹ H. Philip Barber, Appl. Opt. 7, 559 (1968) and references therein.

² E. Gregor, Appl. Opt. 7, 2138 (1968).

³ G. Currie, Appl. Opt. 8, 1068 (1969).

Simple dc Offset Waveform Generator

J. C. TRACY

Science Center, North American Rockwell Corporation,
Thousand Oaks, California 91360

(Received 13 March 1969; and in final form, 24 April 1969)

IN the design of an Auger electron spectrometer a simple scheme was developed for producing a high voltage triangle or ramp waveform offset from ground for the analyzer sweep voltage. The circuit features completely independent control of the dc offset and sweep width. It uses three inexpensive IC operational amplifiers as an offset comparator with hysteresis. The comparator controls a dc motor-driven programming potentiometer of a high voltage supply, which in turn controls the comparator input. This feedback changes the ramp direction at the end points established by the comparator. The linearity is determined by the constancy of the motor speed and the linearity of the programming potentiometer.

The circuit shown in Fig. 1 is for triangle waveforms but the introduction of other bounding circuits at the output of A_1 permits offset ramp generation. The loop consisting of A_1 and A_2 is clearly bistable. Consider the state in which e_z is positive, i.e., A_1 is saturated in the

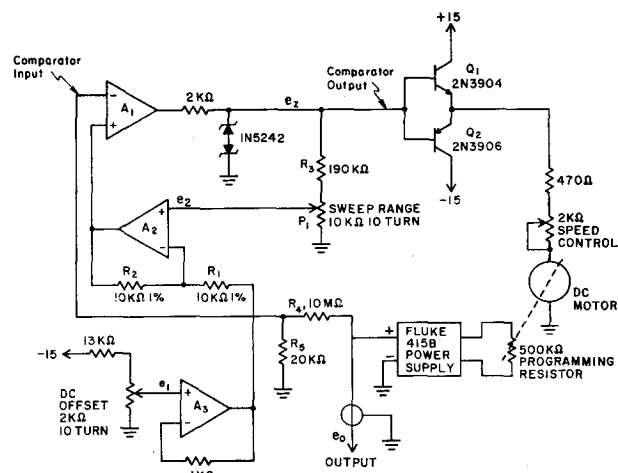


FIG. 1. Schematic diagram of the motor driven sweep circuit. The operational amplifiers are all Fairchild $\mu A741C$ while the motor driven potentiometer is a Beckman model 943.

positive direction. The motor linearly increases the programming resistance causing the power supply output e_o to increase. When the voltage at the inverting input to the comparator, $e_o[R_5/(R_4+R_5)]$, reaches the voltage at the noninverting input of A_1 ,

$$[-e_1(R_1/R_2) + |e_2|(1+R_2/R_1)], \quad (1)$$

the positive loop changes state causing the motor to change direction and the output begins to decrease. When A_1 changes state, e_2 changes sign, so the noninverting input of A_1 then switches to

$$[-e_1(R_1/R_2) - |e_2|(1+R_2/R_1)], \quad (2)$$

establishing the lower end point of the sweep. The voltage e_2 is determined from e_z by R_3 and the setting of P_1 . When this lower limit is reached by the output, the bistable loop changes state again and the process repeats itself.

The sweep width peak-to-peak, e_{sw} , is the difference between (1) and (2) divided by the attenuation of R_4 and R_5 and is equal to

$$e_{sw} = 2(1+R_2/R_1)(1+R_4/R_5)e_2,$$

which is independent of e_1 , while the offset level e_{os} is given by

$$e_{os} = -(R_2/R_1)(1+R_4/R_5)e_1,$$

independent of e_2 . Thus the sweep width is determined uniquely by P_1 while the offset is fixed by P_2 .

The amplifier A_3 serves simply as a unity-gain buffer between the dc offset potentiometer P_1 and the comparator. The bipolar emitter followers Q_1 and Q_2 drive the motor with a maximum current of about 30 mA. The motor-driven pot is a Beckman model 943 with a gear ratio of 500:1, providing a maximum scan rate of about 2 V/sec. Faster scan rates may be obtained simply by choosing lower gear ratios, provided the programmed